
Synthesis and microstructure of gallium substituted cobalt ferrite nanoparticles by hydrothermal method

Gayathri Sivaraman and S. Kalainathan*

Center for Crystal Growth,
VIT University,
Vellore 14, Tamil Nadu, India
Email: gayunaren@gmail.com
Email: kalainathan@yahoo.com
*Corresponding author

Abstract: Magnetic $\text{CoFe}_{2-x}\text{Ga}_x\text{O}_4$ nanoparticles were successfully synthesised via hydrothermal method. The samples were characterised by X-ray diffraction (XRD), field emission scanning electron microscopy (FESEM), transmission electron microscopy (TEM), vibrating sample magnetometer (VSM). The experimental results showed that the $\text{CoFe}_{2-x}\text{Ga}_x\text{O}_4$ were composed of single phase spinel structure and the average crystallite size is between 42 and 57 nm. The saturation magnetisation (Ms) of the $\text{CoFe}_{2-x}\text{Ga}_x\text{O}_4$ nanoparticles decreased linearly as the contents of Ga increased for $x = 0.2-0.8$ which can be used in sensor applications.

Keywords: magnetic nanoparticles; hydrothermal method; field emission scanning electron microscopy; FESEM; HRTEM; VSM magnetic studies.

Reference to this paper should be made as follows: Sivaraman, G. and Kalainathan, S. (2016) 'Synthesis and microstructure of gallium substituted cobalt ferrite nanoparticles by hydrothermal method', *Int. J. Nanoparticles*, Vol. 9, No. 1, pp.11–18.

Biographical notes: Gayathri Sivaraman is a PhD student of VIT University, Vellore, TamilNadu, India. She has completed her VIT University, Vellore, Tamil Nadu, India. She completed her post-graduation from VIT University, Vellore, TamilNadu, India. Her current research interests include magnetic nanoparticles.

S. Kalainathan is a Senior Professor in VIT University, Vellore, Tamil Nadu, India. He has specialisation in the field of crystal growth, NLO materials and nanomaterials.

1 Introduction

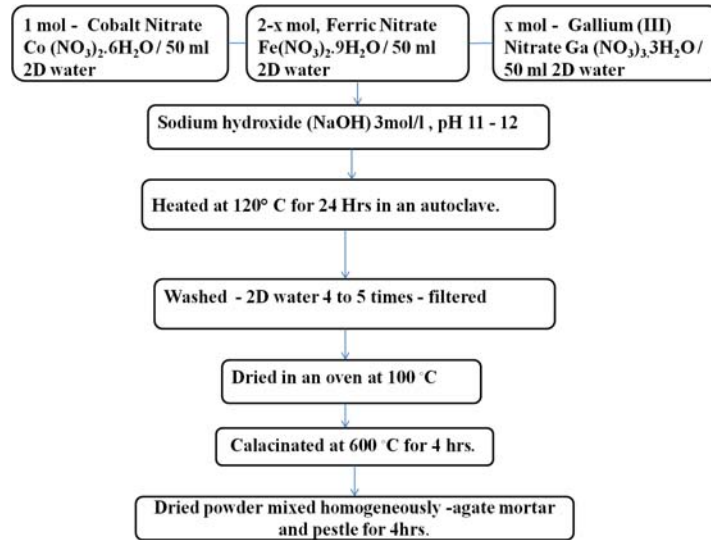
Ferrites general structure $[\text{A}^{2+}]_{\text{tet}} [\text{B}^{3+}]_{\text{octa}} \text{O}_4$ are well known for their electrical, magnetic and catalytic properties (Lo et al., 2005; Koseoglu et al., 2011). In a spinel structured compound AB_2O_4 (A site = divalent cations and B site = trivalent Fe ions) one unit cell contains 32 oxygen atoms that are in direct contact to one another forming a closed-pack face-centred cubic structure with eight tetrahedral (A) and 16 octahedral (B) occupied sites (Kumar and Kar, 2011; Mozaffari et al., 2010). CoFe_2O_4 has an inverse spinel

structure with Co^{2+} ions in the (B) sites and Fe^{3+} ions equally distributed between tetrahedral (A) and octahedral (B) sites. Therefore, by substituting various metal cations change in properties can be observed in these nanoferrites (Patil et al., 2009; Waje et al., 2010). Cobalt ferrite-based composites have high magnetostriction λ , high sensitivity of magnetic induction to applied stress $\text{dB}/\text{d}\sigma$, are chemically very stable and generally of low cost. These factors make these materials attractive for use in magnetoelastic sensors (Chen et al., 1999, 2000). Standard ceramic method has several disadvantages including impurities introduced during the grinding process, poor control of stoichiometric composition, particle-size inhomogeneity, and high sintering temperature. Preparation of ferrites using soft chemistry routes has gained importance due to their advantages in fulfilling the required demands of the processing technologies especially with economic considerations. In Hydrothermal method the chemical reactions occur in aqueous solutions above 100°C under increased pressure, usually equilibrium water pressure. The hydrothermal method can be useful to control grain size, particle morphology, crystalline phase and surface chemistry through regulation of the solution composition, reaction temperature, pressure, solvent properties, additives and aging time (Carp et al., 2004). Song et al. (2007) investigated magnetic properties of a series of Ga-substituted Co ferrites, $\text{CoFe}_{2-x}\text{Ga}_x\text{O}_4$ with x : 0.2–0.8 and found that the magnitude of magnetostriction decreases monotonically while the magnitude of maximum strain derivative $(\text{dk}/\text{dH})_{\text{max}}$ increased for small amount of Ga. They inferred that adjusting Ga content in cobalt ferrite can be a promising route for controlling critical magnetic properties of the material for practical stress sensor applications. No detailed report has been cited in the literature on the structural, electrical and magnetic properties of Ga substituted Co ferrites nanoparticles by hydrothermal method.

2 Experimental procedure

$\text{CoFe}_{2-x}\text{Ga}_x\text{O}_4$ powders with x : 0.2, 0.4, 0.6, 0.8 is prepared by hydrothermal method (Zhang et al., 2010; Khorrami and Manuchehri, 2013) with the aqueous solutions of Co $(\text{NO}_3)_2 \cdot 6\text{H}_2\text{O}$, Fe $(\text{NO}_3)_2 \cdot 9\text{H}_2\text{O}$ and Ga $(\text{NO}_3)_3 \cdot 3\text{H}_2\text{O}$ mixtures, respectively, in alkaline medium. The solutions of Co $(\text{NO}_3)_2 \cdot 6\text{H}_2\text{O}$, Fe $(\text{NO}_3)_2 \cdot 9\text{H}_2\text{O}$ and Ga $(\text{NO}_3)_3 \cdot 3\text{H}_2\text{O}$ in their stoichiometry (0.1M of Co $(\text{NO}_3)_2 \cdot 6\text{H}_2\text{O}$ in 100 ml, 0.18M of Fe $(\text{NO}_3)_2 \cdot 9\text{H}_2\text{O}$ in 100 ml, 0.02M of Ga $(\text{NO}_3)_3 \cdot 3\text{H}_2\text{O}$ in 100 ml in the case of $x = 0.2$ ($\text{CoFe}_{1.8}\text{Ga}_{0.2}\text{O}_4$) and similarly for other values of (x) were dissolved in double distilled water with a constant stirring. The pH maintained was between 11~12 using NaOH solution. The prepared mixed solution was transferred in to a 250 ml Teflon lined stainless autoclave. The autoclave was sealed and treated at 120°C for 24 hours. After the hydrothermal reaction time, the autoclave was taken out and the autoclave was cooled to room temperature naturally. The samples obtained were washed four to five times with deionised water and ethanol. A general flow chart of synthesis process is shown in Figure 1. The product was dried in hot air oven at 100°C for overnight to remove moisture. The dried powder was mixed homogeneously in an agate mortar and pestle for 2 hours. This homogenous mixture was sintered at 600°C for 6hrs in a hot air furnace and again the grinding was repeated.

Figure 1 Flow chart for synthesis process of $\text{CoFe}_{2-x}\text{Ga}_x\text{O}_4$ nanoparticles using hydrothermal method (see online version for colours)



3 Measurements

X-ray powder diffraction analysis was carried out on Bruker, D8 Advance model diffractometer [X-ray diffraction, (XRD)] using $\text{Cu K}\alpha$.

Field emission scanning electron microscope (FE-SEM with EDX using Carl Zeiss SUPRA-555) was used to investigate the surface morphology and the elemental composition of the samples. The samples were all coated with carbon prior to SEM analysis.

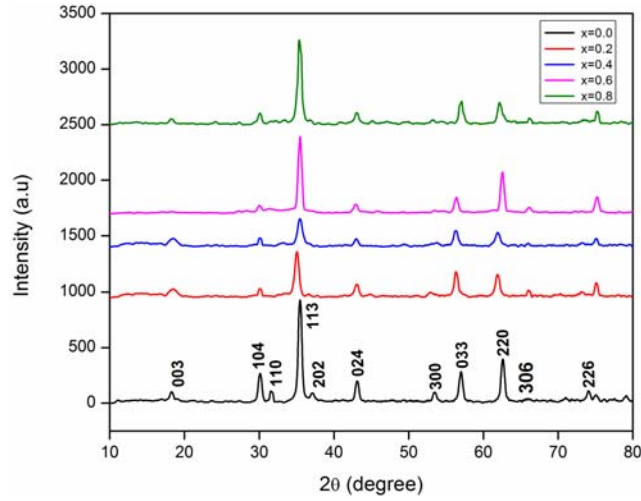
The nanoparticles morphology of the annealed samples was confirmed using high resolution tunnelling electron microscope (HR-TEM) PHILIPS, Model: CM200.

Room temperature magnetic measurement of the samples was carried out with vibrating sample magnetometer (VSM). The parameters like saturation magnetisation (M_s), coercive force (H_c) and remanent magnetisation (M_r) were evaluated.

4 Result and discussion

4.1 XRD analysis

The powder XRD pattern of $\text{CoFe}_{2-x}\text{Ga}_x\text{O}_4$ for x : 0.2, 0.4, 0.6 and 0.8 by the hydrothermal method is shown in Figure 2 in which it is confirmed that all the samples have a cubic spinel structure. The average crystallite size for each composition was calculated using the Scherrer formula (Culity, 1978) and found that the particle size increases with increasing concentration of gallium in cobalt ferrite from 42 nm for $x = 0.2$ to 57 nm for $x = 0.8$.

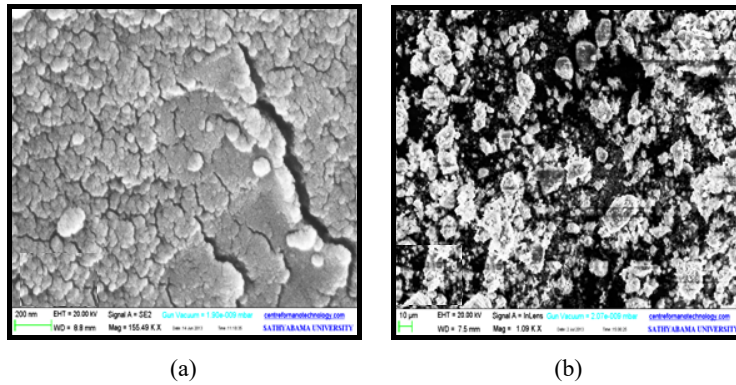
Figure 2 X-ray diffraction patterns of $\text{CoFe}_{2-x}\text{Ga}_x\text{O}_4$ system by hydrothermal method (see online version for colours)

4.2 Structural analysis

Figure 3 shows the FESEM of the $\text{CoFe}_{2-x}\text{Ga}_x\text{O}_4$ ferrite samples studied in the present work. The average grain size was determined using the linear intercept method (Postupolski, 1988) estimated using the relation

$$G_{avg} = 1.5L/(M \times N)$$

where L is the total test line length, M is the magnification and N is the total number of interception for all the sample and the values are presented in Table 1. It is evident from Table 1 that the grain size of all the samples is in nanometer dimension.

Figure 3 FESEM images of $\text{CoFe}_{2-x}\text{Ga}_x\text{O}_4$ system (a) $x = 0.2$ and (b) $x = 0.8$ (see online version for colours)

(a)

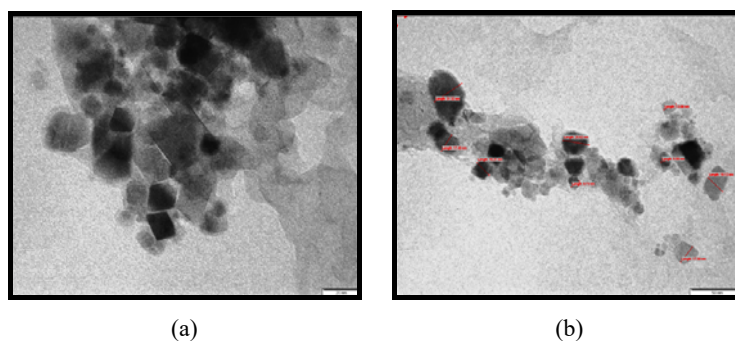
(b)

Table 1 Saturation magnetisation (M_s), remanence magnetisation (M_r), coercivity (H_c), remanence ratio (M_r/M_s), anisotropy constant (K), of $\text{CoFe}_{2-x}\text{Ga}_x\text{O}_4$ system

Composition	Crystalline size (nm)	M_s (emu/g)	M_r (emu/g)	H_c (Oe)	M_r/M_s	K (erg/Oe) 10^{-4}
CoFe_2O_4	66	56	22.27	1,095.17	0.3976	62.581
$\text{CoFe}_{1.8}\text{Ga}_{0.2}\text{O}_4$	42	45.54	16.02	809.49	0.3518	37.616
$\text{CoFe}_{1.6}\text{Ga}_{0.4}\text{O}_4$	46	26.12	7.42	590.97	0.284	15.751
$\text{CoFe}_{1.4}\text{Ga}_{0.6}\text{O}_4$	53	20.23	3.902	486.98	0.1928	10.052
$\text{CoFe}_{1.2}\text{Ga}_{0.8}\text{O}_4$	57	48.12	13.36	274.56	0.2776	13.481

4.3 TEM analysis

A TEM micrograph produces high resolution, black and white images due to the interaction of prepared sample and energetic electrons in the vacuum chamber. The TEM micrograph of $\text{CoFe}_{1.2}\text{Ga}_{0.8}\text{O}_4$ by hydrothermal method is shown in Figure 4. As can be seen the distribution of the particles is mostly uniform and their shape is almost spherical.

Figure 4 TEM micrographs of $\text{CoFe}_{1.2}\text{Ga}_{0.8}\text{O}_4$ (see online version for colours)

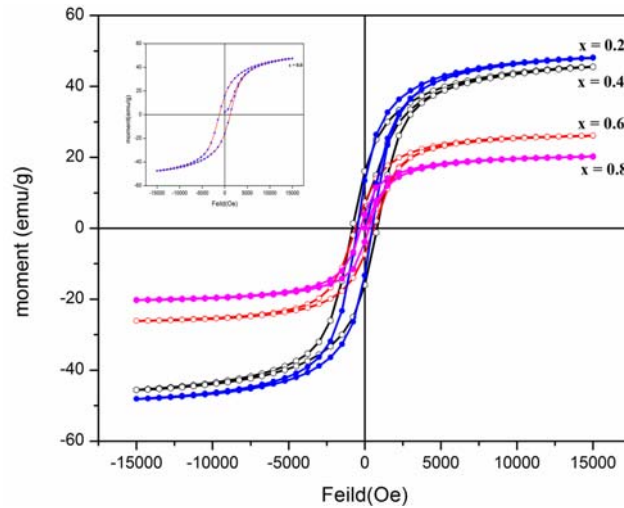
4.4 VSM analysis

The room temperature hysteresis loops for $\text{CoGa}_x\text{Fe}_{2-x}\text{O}_4$ samples ($x = 0.2, 0.4, 0.6$ and 0.8) which were calcinated at 600°C are shown in Figure 5, the inlet of the Figure 5 shows the hysteresis loop of pure CoFe_2O_4 nanoparticles. The substitution of nonmagnetic ion Gallium, which has a preferentially A site occupancy results in the reduction of the exchange interaction between A and B sites. Hence, by varying the Ga content, it is possible to vary magnetic properties of the nanoparticles. The saturation magnetisation (M_s), remanent magnetisation (M_r) and coercivity (H_c) values are listed in Table 1 for the given samples. The saturation magnetisation (M_s) decreases with increase of crystallite size. According to Kim and Shima (2007), there are two possible models to explain the decrease of M_s as the content of Ga^{3+} increases: the surface spin disorder model and the uniformly reduced magnetic moment model. For the as-prepared $\text{CoGa}_x\text{Fe}_{2-x}\text{O}_4$ nanoparticles, the decrease of M_s with increasing Gallium content is caused by the higher magnetic moment of Co^{2+} than Ga^{3+} at octahedral sites in the inverse spinel structure (Qi et al., 2010). Alignment of number of atomic spins along with

the applied magnetic field increases with the increase of magnetic domain, which leads to enhancement of the saturation magnetisation with the crystallite size (Patil et al., 2009). For $\text{CoGa}_x\text{Fe}_{2-x}\text{O}_4$ bulk samples, the saturation magnetisation gradually increased up to $x = 0.4$ and then decreased for higher x content (Bhattacharya and Darshane, 1993; Ranvah et al., 2008). In the case of $\text{CoGa}_x\text{Fe}_{2-x}\text{O}_4$ nanoparticles for low Ga substitution, Ga^{3+} ions appear in the tetrahedral site. While at high Ga concentration, Ga^{3+} preferred the octahedral site. This indicates that Ga^{3+} ions substitute Fe^{3+} in A- and B-sites. The value of coercivity H_c decreases with increase in Ga^{3+} concentration. A decrease in coercivity with increase in gallium concentration may be attributed to the decrease in anisotropy field, which in turn decreases the domain wall energy (Yakovlev et al., 1969; Gul et al., 2007) or decrease of the crystallite size (Kumar et al., 2013). From the values of coercivity H_c and the saturation magnetisation M_s the value of anisotropy constant can be calculated using the relation (Wahba and Mohamed, 2014).

$$H_c = 0.98 K/M_s.$$

Figure 5 Hysteresis loop for pure CoFe_2O_4 (inset) and $\text{CoFe}_{2-x}\text{Ga}_x\text{O}_4$ by hydrothermal method (see online version for colours)



The variation of anisotropy constant, K with Ga^{3+} concentration is shown in Table 1. The change in K value could be caused by either of two mechanisms (Ranvah et al., 2008):

- 1 according to the one-ion anisotropy model, the high anisotropy of cobalt ferrite is primarily due to the presence of Co^{2+} ions on the octahedral sites of the spinel structure
- 2 the present of Ga^{3+} in tetrahedral site decreases the anisotropy due to the reduction of the tetrahedral-octahedral exchange coupling.

Hence, we observe that the M_s , M_r and H_c values obtained for the $\text{CoGa}_x\text{Fe}_{2-x}\text{O}_4$ nanoparticles are less than that of the values obtained by Song et al. (2007) in bulk growth.

5 Conclusions

The nanoparticles of $\text{CoGa}_x\text{Fe}_{2-x}\text{O}_4$ were synthesised by hydrothermal method. The size of the nanoparticles is in the range of 42–57 nm which are in good agreement with the values obtained by XRD, SEM and TEM indicating that there are no agglomerations. The saturation magnetisation (M_s), remanent magnetisation (M_r) and coercivity (H_c) decreases with an increase in Ga content. The saturation magnetisation (M_s) decreases due to increase in the crystallite size. The M_s , M_r , H_c values obtained for $\text{CoGa}_x\text{Fe}_{2-x}\text{O}_4$ nanoparticles are less than the values obtained by bulk method. This property makes the $\text{CoGa}_x\text{Fe}_{2-x}\text{O}_4$ to play a vital role in sensor devices applications.

References

- Bhattacharya, U. and Darshane, V.S. (1993) 'Spin-glass behaviour of the system $\text{CoFe}_{2-x}\text{Ga}_x\text{O}_4$ ', *J. Mater. Chem.*, Vol. 3, Nos. 1–2, p.299.
- Carp, O., Huisman, C.L. and Reller, A. (2004) 'Photoinduced reactivity of titanium dioxide', *Progress in Solid State Chem.*, Vol. 32, Nos. 1–2, pp.33–177.
- Chen, Y., Snyder, J.E., Dennis, K.W., McCallum, R.W. and Jiles, D.C. (2000) 'Temperature dependence of the magnetomechanical effect in metal-bonded cobalt ferrite composites under torsional strain', *J. Appl. Phys.*, Vol. 87, No. 5789, pp.5798–5800.
- Chen, Y., Snyder, J.E., Schwichtenberg, C.R., Dennis, K.W., McCallum, R.W. and Jiles, D.C. (1999) 'Metal-bonded Co-ferrite composites for magnetostrictive torque sensor applications', *IEEE Trans. Magn.*, Vol. 35, No. 3652, p.EF06.
- Culity, B.D. (1978) *Elements of X-ray Diffraction*, 2nd ed., Addison-Wesley Series, Reading, Massachusetts.
- Gul, I.H., Abbasi, A.Z., Amin, F., Anis-ur-Rehman, M. and Maqsood, A. (2007) 'Structural, magnetic and electrical properties of $\text{Co}_{1-x}\text{Zn}_x\text{Fe}_2\text{O}_4$ synthesized by co-precipitation method', *J. Magn. Mater.*, Vol. 311, No. 2, p.494.
- Khorrani, S.A. and Manouchehri, Q.S. (2013) 'Magnetic properties of cobalt ferrite synthesized by hydrothermal and co-precipitation methods: a comparative study', *Journal of Applied Chemical Research*, Vol. 7, No. 3, pp.15–23.
- Kim, T. and Shima, M. (2007) 'Reduced magnetization in magnetic oxide nanoparticles', *Journal of Applied Physics*, Vol. 101, No. 9, p.09M516.
- Koseoglu, Y., Bay, M., Tan, M., Baykal, A., Sozeri, H., Topkaya, R. and Akdogan, N. (2011) 'Magnetic and dielectric properties of $\text{Mn}_{0.2}\text{Ni}_{0.8}\text{Fe}_2\text{O}_4$ nanoparticles synthesized by PEG-assisted hydrothermal method', *J. Nanopart. Res.*, Vol. 13, No. 5, pp.2235–2244.
- Kumar, L. and Kar, M. (2011) 'Influence of Al^{3+} ion concentration on the crystal structure and magnetic anisotropy of nanocrystalline spinel cobalt ferrite', *Journal of Magnetism and Magnetic Materials*, Vol. 323, No. 15, pp.2042–2048.
- Kumar, L., Kumar, P. and Kar, M. (2013) 'Effect of non-magnetic substitution on the structural and magnetic properties of spinel cobalt ferrite ($\text{CoFe}_{2-2x}\text{Al}_x\text{O}_4$) ceramics', *J. Mater. Sci.: Mater. Electron.*, Springer Science+Business Media New York [online] DOI 10.1007/s10854-013-1159-5 (accessed 22 February 2013).
- Lo, C.C.H., Ring, A.P., Snyder, J.E. and Jiles, D.C. (2005) 'Improvement of magneto mechanical properties of cobalt ferrite by magnetic annealing', *IEEE Trans. Magn.*, Vol. 41, No. 10, pp.3676–3678.
- Mozaffari, M., Manouchehri, S., Yousefi, M.H. and Amighian, J. (2010) 'The effect of solution temperature on crystallite size and magnetic properties of Zn substituted Co ferrite nanoparticles', *Journal of Magnetism and Magnetic Materials*, Vol. 322, No. 4, pp.383–388.

- Patil, V.G., Shirsath, S.E., More, S.D., Shukla, S.J. and Jadhav, K.M. (2009) 'Effect of zinc substitution on structural and elastic properties of cobalt ferrite', *J. Alloys Compd.*, Vol. 488, No. 1, pp.199–203.
- Patil, V.G., Shirsath, S.E., More, S.D., Shukla, S.J. and Jadhav, K.M. (2009) 'Effect of zinc substitution on structural and elastic properties of cobalt ferrite', *J. Alloys Compd.*, Vol. 488, No. 1, pp.199–203.
- Postupolski, T. (1988) 'Prace inst. teledi radio', *Zesz.*, Vol. 87, No. 1, p.107.
- Qi, Y.L., Yang, Y.S., Zhao, X.F. et al. (2010) 'Controllable magnetic properties of cobalt particles derived from layered double hydroxide precursors', *Particuology*, Vol. 8, No. 9, pp.207–211.
- Ranvah, N., Melikhov, Y., Jiles, D.C., Snyder, J.E., Moses, A.J., Williams, P.I. and Song, S.H. (2008) 'Temperature dependence of magnetic anisotropy of Ga-substituted cobalt ferrite', *J. Appl. Phys.*, Vol. 103, No. 7, p.07E506.
- Song, S.H., Lo, C.C., Lee, S.J., Aldini, S.T. and Snyder, J.E. (2007) 'Magnetic and magnetoelastic properties of Ga-substituted cobalt ferrite', *J. Appl. Phys.*, Vol. 101, No. 9, No. 09C517.
- Wahba, A.M. and Mohamed, M.B. (2014) 'Structural, magnetic, and dielectric properties of nanocrystalline Cr-substituted $\text{Co}_{0.8}\text{Ni}_{0.2}\text{Fe}_2\text{O}_4$ ferrite', *Ceram. Int.*, Vol. 40, No. 4, p.6127.
- Waje, S.B., Hashim, M., Yousoff, W.D.W. and Abbas, Z. (2010) 'Sintering temperature dependence of room temperature magnetic and dielectric properties of $\text{Co}_{0.5}\text{Zn}_{0.5}\text{Fe}_2\text{O}_4$ prepared using mechanically alloyed nanoparticles', *J. Magn. Magn. Mater.*, Vol. 322, No. 6, pp.686–691.
- Yakovlev, Y.M., Rubalikaya, E.V. and Lapovok, N. (1969) 'Ferromagnetic resonance in lithium ferrite', *Sov. Phys. Solid State*, Vol. 10, No. 6, p.2301.
- Zhang, Y., Liu, Y., Fei, C., Yang, Z. and Lu, Z. (2010) 'The temperature dependence of magnetic properties for cobalt ferrite nanoparticles by the hydrothermal method', *J. Appl. Phys.*, Vol. 108, No. 8, pp.193904-1–193904-7.